2011 American Control Conference
on O'Farrell Street, San Francisco, CA, USA
June 29 - July 01, 2011

Flow-Capacity-Maintaining, Decentralized, Conflict Resolution with Aircraft Turn Dynamics

Jeff Yoo and Santosh Devasia
Department of Mechanical Engineering, University of Washington

Abstract— **This article presents a decentralized conflict resolution procedure (CRP) that maintains the flow capacity in each of two intersecting routes. The main contribution of this article is the development of CRPs that include the effect of aircraft, turn dynamics that limits the heading-change rate.**

I. Introduction

This article presents a decentralized, conflict resolution procedure (CRP), which can be shown to be provably safe, for enroute Air Traffic Control (ATC), . It is noted that CRPs tend to be decentralized (spatially-and-temporally) because of a substantial increase in computational and modeling complexity with a centralized CRP when the number of aircraft (and conflicts) increase. Additionally, centralized controllers become inefficient, over large airspace, because of the need to handle the uncertainty in aircraft trajectories over time, e.g., because of ground-speed sensitivity to wind and temperature [1] that depend on forecasts of dynamic weather conditions with substantial uncertainties [2]. Therefore, decentralized CRPs are needed to resolve conflicts to manage the complexity and uncertainty in air traffic control. A major challenge, however, is to ensure that modifications of flight trajectories, for resolving a conflict, do not lead to a *domino* effect; i.e., resolution of a conflict should not lead to new conflicts, whose resolution leads to additional conflicts, and so on [3]. Moreover, the procedure should always lead to a solution of the conflict resolution problem for guaranteeing safety. Thus, developing provably-safe, decentralized CRPs remains an important issue in air traffic control, which is addressed in this article.

Previous works on CRPs range from non-local probabilistic approaches that handle uncertainties [4] to local deterministic approaches that resolve conflicts in a collaborative manner [5], [6]. Analytical issues such as proving local safety of conflict resolution were studied in, e.g., Ref. [7]. The problem of guaranteed conflict resolution in a stable manner remains more challenging for the non-local case. For example, procedures to resolve conflicts between aircraft along two intersecting routes might not be stable when multiple aircraft arrive along the route as shown in Ref. [8]. Conditions for CRP stability were studied, for two and three intersecting routes, in Refs. [6], [8]. The main difficulty is that conflict resolution at one routes intersection will interact with the conflict resolution at the next intersection in the sequence; stable solutions to the resulting coupled problem tends to require centralized solutions [8]. In contrast, the current work seeks decentralized procedures that guarantee conflict resolution with multiple conflicts (intersections) by using decoupled, conflict-resolution procedures — the cost of this guarantee is time delay in the flow, however, with known bounds.

Recent work [9] has identified sufficient and necessary conditions for general decentralized conflict resolution procedures (CRPs) with guaranteed safety when aircraft are in pre-specified *highway-like* routes as in Refs. [10], [11]. The main idea is to design CRPs that that resolve conflicts while maintaining in each route: (i) the flow capacity; (ii) the aircraft sequence; and (iii) the required spacing between aircraft [9]. This approach decouples the aircraft flow in each route from the CRP, and therefore, the CRP at the next intersection (along a route) can be designed independent of the current CRP. Moreover, since the proposed CRPs do not require a reduction of the flow capacity, they can aid in increasing the efficiency of enroute Air Traffic Control (ATC), e.g., in the design of capacity-maintaining protocols for adverse weather re-routing as discussed in Ref. [10]. However, the initial design of provably-safe CRP in Ref. [10] does not limit the rate of heading angle change, i.e., the heading angle is assumed to change instantly. The main contribution of the current article is to develop decentralized CRPs which include the effects of turn dynamics by limiting the heading-change rate allowed in the CRP. The redesigned CRP satisfies the decoupling conditions in Ref. [9], and can therefore be used to develop provably-safe decentralized CRPs.

II. The Conflict Resolution Procedure (CRP)

A. Airspace and Conflict Description

The conflict resolution procedure is studied for two perpendicularly intersecting aircraft routes (R_1 and R_2), which are assumed to be at a fixed altitude (planar flight) as illustrated in Fig 1. A sufficiently-large local region L around the intersection (conflict point CP) is assumed to be conflict free from all other routes in the airspace. The CRP can use this local region L to resolve conflicts at the intersection without potentially causing additional conflicts as long as the rerouting procedures in the CRP are within the local region L, and the conflict points are sufficiently sparse in the airspace. Aircraft along the nominal routes (R_1 and R_2) arrive into this local region L at arrival points A_1, A_2 with a fixed nominal speed v_{sp} and exit at E_1, E_2 as shown in Fig. 1. It is assumed that aircrafts, arriving at the local region L are separated by at least distance $\overline{D}$ at the arrival points

978-1-4577-0079-8/11/$26.00 ©2011 AACC

A_1, A_2, where the minimal arrival spacing $\overline{D}$ is greater than the minimum required separation distance D_{sep} to avoid conflicts.

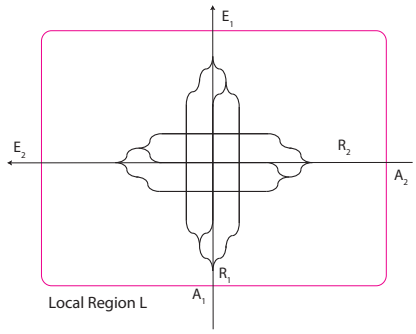

Fig. 1. Local region L of the airspace around two perpendicularly intersecting routes. Associated with these two routes R_1, R_2 are arrival points A_1, A_2, and exit points E_1, E_2 respectively.

***Remark** 1:* In general, conflict resolution can be achieved using maneuvers that change the heading, speed and altitude. However, heading changes are preferred over speed changes, which require additional fuel for accelerating and decelerating the aircraft. Similarly, heading changes are preferred over altitude changes, which tend to incur passenger discomfort and can cause conflicts in the other altitudes [6].

***Remark** 2:* If the intersection angle between two routes are non-perpendicular, then the routes could be turned to create a perpendicular intersection before the current approach is applied.

B. The Conflict Resolution Problem

This article studies heading-change-based conflict resolution procedures (CRPs). The requirements on each decentralized CRP, to enable decoupled designs, are stated below.

***Definition** 1:* [**CRP Decoupling Conditions**] The problem is to find a conflict resolution procedure (CRP) using heading change maneuvers (with limits on the rate of heading change) such that conflicts are avoided between aircraft and the following CRP-decoupling conditions are satisfied:

1) **local intent** aircraft on each route (R_1, R_2) exit along the same route at the corresponding exit point E_1, E_2;
2) **local liveness** aircraft on each route exit the local region L within a specified bounded maximum time $T < \infty$;
3) **local fairness** the passage through the local region L is on a first-come-first-served (FCFS) basis within each route; and
4) **local exit spacing** aircraft exiting the local region L (at each of the two exit points) are separated by at-least distance $\overline{D}$.

***Remark** 3:* The local liveness and fairness conditions are not required for safety of the CRPs; however, liveness implies that aircraft will not be stuck in the airspace (e.g., in a loop) and fairness enables acceptance of the conflict resolution procedure. The first-come-first-served (FCFS) scheduling of aircraft through the airspace is considered as the canonical, fair schedule in Air Traffic Management [12].

C. Proposed CRP

In general, if the aircraft are closely spaced in each route, then there is insufficient space to pass the aircraft from the two routes through a single intersection point. Therefore, the main route needs to be split (using diverge procedures) into multiple paths to increase the spacing between aircraft (in each path). Aircraft in these paths can then intersect without conflicts (provided the aircraft motions are synchronized as shown in Refs. [9]); after the intersections, the paths can be merged back to the main routes.

CRP with a Three Path Split: The proposed conflict resolution procedure (CRP) is shown in Fig. 2 — it consists of splitting of each route (R_1, R_2) into three equal-length paths and choosing one of the paths for each arriving aircraft. In particular, the three paths $\{R_{1,i}\}_{i=1}^{i=3}$ for route R_1 (shown in Fig. 2) are described by a set of way points (v_i):

$$\begin{aligned} R_{1,1} &= \{v_1, v_2, v_3, v_4, v_5, v_6, v_7, v_8, v_9\} \\ R_{1,2} &= \{v_1, v_{16}, v_{17}, v_{18}, v_{19}, v_{20}, v_{21}, v_{15}, v_9\} \\ R_{1,3} &= \{v_1, v_2, v_{10}, v_{11}, v_{12}, v_{13}, v_{14}, v_{15}, v_9\}, \end{aligned} \quad (1)$$

and the three paths $\{R_{2,i}\}_{i=1}^{i=3}$ for route R_2 are

$$\begin{aligned} R_{2,1} &= \{v_{22}, v_{23}, v_{25}, v_{18}, v_{11}, v_4, v_{28}, v_{31}, v_{33}\} \\ R_{2,2} &= \{v_{22}, v_{23}, v_{26}, v_{19}, v_{12}, v_5, v_{29}, v_{32}, v_{33}\} \\ R_{2,3} &= \{v_{22}, v_{24}, v_{27}, v_{20}, v_{13}, v_6, v_{30}, v_{32}, v_{33}\}. \end{aligned} \quad (2)$$

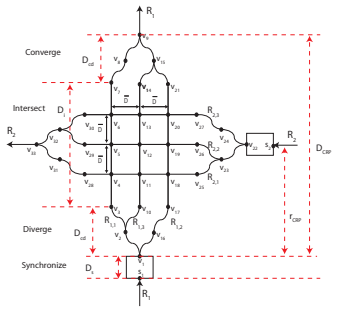

Fig. 2. Overview of actions in the conflict resolution algorithm: (i) synchronize; (ii) diverge; (iii) intersect; and (iv) converge. Way-points v are numbered along paths $R_{1,1}, R_{1,3}, R_{1,2}$ for route R_1 and then along the paths for route R_2 (from left to right, bottom to top). The paths have the same lengths

Path Assignment for each Route: The path assignment procedure is illustrated in Fig. 3; the procedure is based on the index k in the scheduled time of arrival (STA) t_k at the initial way-points (v_1 or v_{22} along Routes R_1, R_2 as in Fig. 2), which are assumed to be discrete time instants. Synchronization procedures are needed to achieve the scheduled time of arrivals (STAs); however, achieving STAs has been well studied in the literature, e.g., to schedule arrivals at airports as in Ref. [12]. Such approaches can be adapted to achieve STAs at the conflict point [9], and is therefore, not discussed in this article.

***Definition** 2:* [**Path Assignment Procedure**] Let the scheduled time of arrival (STA) of aircraft at the initial way-points (v_1 for route R_1 and v_{22} for route R_2 in Fig. 2) be at discrete time instants t_k

$$t_k \quad = k\left(\frac{\overline{D}/2}{v_{sp}}\right) \quad = kT_{\overline{D}/2} \tag{3}$$

where k is a nonnegative even integer for route R_1 and a nonnegative odd integer for route R_2. Then, if STA k is even (i.e., aircraft is on route R_1 arriving at way-point v_1) then assign path $R_{1,j+1}$ where j is $k/2$ modulus 3. If k is odd (i.e., aircraft is on route R_2 at way-point v_{22}) then assign path $R_{2,j+1}$ where j is $(k-1)/2$ modulus 3, as illustrated in Fig. 3.

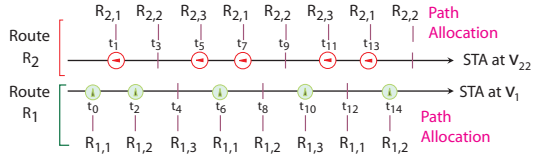

Fig. 3. Path allocation: each aircraft is assigned a path based on its scheduled time of arrival STA.

***Remark** 4:* The time difference, $2T_{\overline{D}/2}$ in Eq. (3), between two scheduled time of arrivals (STAs) on a single route, corresponds to the time needed to travel (with nominal speed v_{sp}) the minimum separation distance $\overline{D}$ between aircraft arriving in each route.

***Remark** 5:* The path allocation rule is cyclic and repeats after every six discrete time instants.

D. CRP satisfies Decoupling Conditions

***Lemma** 1:* The CRP satisfies the decoupling conditions in Definition 1 provided: (i) the aircraft arrival can be synchronized to the discrete time instants as in Fig. 3; and (ii) the CRP avoids conflicts.

Proof: The CRP maintains the same aircraft sequence (local fairness) as at the arrival way-points (v_1 for route R_1 and v_{22} for route R_2 in Fig. 2) since the path lengths are the same. Since the paths for each route merge back to that route, local intent is satisfied, and the finiteness of the path length implies that the time needed to merge back to the route only takes a finite amount of time (local liveness). The discrete arrival times implies that the aircraft arrive with a minimal spacing of $\overline{D}$ — the spacing is maintained at the exit as the aircraft merge back at the end of the CRP since the path lengths are the same and the nominal speed is constant. ■

E. CRPs are Decoupled and Maintain Route-Flow Capacity

The CRP does not change the sequence of aircraft in each route and maintains a minimal separation of $\overline{D}$ (i.e., the route-flow capacity for which the CRP is designed) at the exit. Therefore, if aircraft in one of the routes (R_1 or R_2) reaches another conflict point then the CRP at the second intersection point does not have to depend on the procedures used at the first CRP provided the conflict points are sufficiently separated from each other, i.e., the associated local regions needed for conflict resolution are disjoint. Thus, the design of the proposed distributed CRPs (that only used local information of each route) can be decoupled from each other, without domino-type stability problems if the conflict points are sufficiently sparse in the airspace.

III. Conditions for Conflict Avoidance

The design of the CRP in Fig. 2 to avoid conflict between aircraft is studied in this section. The section begins with (i) the diverge procedure and is followed by (ii) the intersect procedure. It is noted that the converge procedure is the same as the diverge procedure backwards in time, and hence shares the same conflict avoidance issues — the issues in the converge procedure are therefore not discussed to avoid repetition.

A. Diverge Procedure

The diverge procedure splits the routes into paths (i) without conflicts, and (ii) without losing synchronization in the different paths, by using equal length maneuvers.

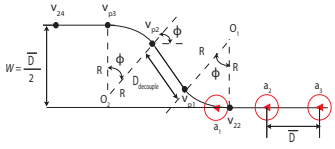

Fig. 4. Detail of path $R_{2,3}$ in Fig. 2 showing two turns from node v_{22} to v_{24}

Potential for Conflicts during Turns: A critical concern is that the spacing between aircraft along a route could decrease during a turn (when compared to the arrival spacing $\overline{D}$ along each straight route) and result in the loss of minimum separation. Turns occur during the diverge procedure, for example, in the path $R_{2,3}$, the route segment from v_{22} to v_{24} (diverge) consists of two consecutive turn paths each with constant radius R, and each curved path results in a heading angle change of ϕ as shown in Fig. 4. The potential for reduction in aircraft spacing during a turn places a lower limit on the initial spacing ($\overline{D}$) to achieve a turn ϕ without conflict. These restrictions can become more stringent when making consecutive turns, e.g., from way-point v_{22} to v_{24} on route $R_{2,3}$ in Fig. 4. Conditions for conflict-free turns are studied below for two cases: (i) single turn; and (ii) consecutive turns. This section begins by considering the restrictions on the rate of heading change.

Restriction on Heading-Change Rate: Although the roll dynamics is relatively fast and can be ignored in the CRP path design, the aircraft turn dynamics should be included in terms of an upper bound on the heading-change rate $\dot{\theta}$ as in Ref. [13]. In particular, from the free body diagram of the aircraft (in the vertical plane) shown in Fig. 5,

$$L\cos(\mu) = mg; \qquad L\sin(\mu) = m\frac{v_{sp}^2}{R}, \tag{4}$$

where μ represents the bank angle, v_{sp} is the nominal speed m is the aircraft mass and g is the gravitational acceleration. Then, the turn radius is given by (from Eq. 4)

$$R = \frac{v_{sp}^2}{g\tan(\mu)}. \tag{5}$$

With a bank angle limit of $\mu \leq \mu_{max}$ (with $\mu_{max} = 30°$ for passenger safety and comfort in commercial aircraft [13]), the minimum turn radius R_{min} is given by

$$R_{min} = \frac{v_{sp}^2}{g\tan(\mu_{max})}. \tag{6}$$

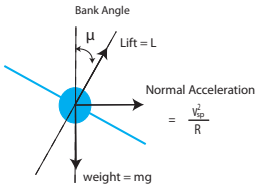

Fig. 5. Free body of aircraft performing a banked turn; the limit on the acceptable bank angle limits the maximum heading-change rate.

The above lower bound on the turn radius, i.e., $R > R_{min}$, leads to an upper bound on the maximum heading-change rate. Let the aircraft make a heading change of $\theta \leq \phi$ in time t along a circular arc of radius R and length

$$R\theta \ = v_{sp}t,$$

as shown in Fig. 6. Then, the upper bound on the heading-change rate is obtained as

$$\dot{\theta} \ = \ \frac{v_{sp}}{R} \quad \leq \ \frac{v_{sp}}{R_{min}} \quad = \frac{g\tan(\mu_{max})}{v_{sp}} \ = \Omega_{max}. \tag{7}$$

Note that the rate of heading change $\dot{\theta}$ can be kept below the limit of Ω_{max} by choosing a sufficiently large turn radius R, i.e.,

$$R \ \geq \ R_{min} \ = \frac{v_{sp}}{\Omega_{max}}. \tag{8}$$

Thus, the limit on the acceptable bank angle (in the turn dynamics) limits the maximum heading-change rate to a maximum-rate of Ω_{max}.

Single Turn Analysis: Consider a single turn in a route where aircraft start from a straight section, then move along a circular arc of length $R\phi$, and finally continue along a straight line — both the straight line segments are tangential to the circular arc and the angle between the two straight segments correspond to ϕ as shown in Fig. 6.

***Lemma 2 (*Single Turn):** To avoid conflict between aircraft on the route with the single curved turn (as in Fig. 6 with $R > R_{min}$) with a maximum heading change of $\phi \leq \pi/2$, the minimum separation distance $\overline{D}$ between arriving aircraft (on the straight segment) should satisfy

$$\overline{D} \ \geq \ \frac{D_{sep} - 2R\sin(\frac{\phi}{2})}{\cos(\frac{\phi}{2})} + R\phi \quad \text{if} \quad \phi \leq \phi^* = \frac{\overline{D}}{R} \tag{9}$$

and

$$\overline{D} \ \geq \ 2R\sin^{-1}\left(\frac{D_{sep}}{2R}\right) \quad \text{if} \quad \phi \geq \phi^* \tag{10}$$

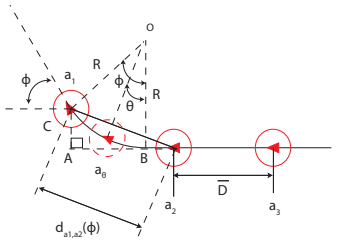

Fig. 6. Single curved-turn case.

where the two conditions are equivalent at the critical angle when $\phi = \phi^*$. Turn angle ϕ less than ϕ^* will be referred to as scenario 1 and turn angle ϕ greater than ϕ^* will be referred to as scenario 2 .

Proof: The proof is divided into four steps.

Step 1: Distance decreases during the turn The distance between the forward aircraft a_1 and an aft aircraft a_2 that were separated by distance $\overline{D}$ in the straight portion decreases as aircraft a_1 starts turning along the circular arc, while the aft aircraft a_2 is still on the straight path as in Fig. 6. To show this, consider the distance d_{a_1,a_2} between the two aircraft when the heading change of $\phi \leq \phi^*$ is completed by the first aircraft a_1 as in Fig. 6 given by

$$d_{a_1,a_2}(\phi) \ = \ \sqrt{(\overline{D} - R\phi + R\sin\phi)^2 + (R - R\cos\phi)^2} \quad \text{if} \quad \phi \leq \phi^* \tag{11}$$

which follows from the right angled triangle a_1Aa_2 because the length of the arc Ba_1 is $R\phi$, path distance between the two aircraft is $\overline{D}$ due to the constant speed assumption, and thereby, the distance $d_{B,a2}$ is $\overline{D} - R\phi$. If the turn angle θ completed by the aircraft a_1 satisfies $0 < \theta < \phi \leq \phi^*$, then the same expression holds with ϕ replaced by θ, i.e.,

$$d_{a_1,a_2}(\theta) = \sqrt{(\overline{D} - R(\theta - \sin\theta))^2 + (R - R\cos\theta)^2} \tag{12}$$

with the derivative of the distance-squared given by

$$\begin{aligned} \tfrac{d}{d\theta}[d_{a_1,a_2}(\theta)]^2 \ &= \ -2R\left(\overline{D} - R\theta\right)(1 - \cos\theta) \\ &< \ 0 \quad \text{if } \theta \leq \phi < \phi^* \quad \text{and} \quad \phi \leq \pi/2 \end{aligned} \tag{13}$$

because $\overline{D} = R\phi^* \geq R\theta$ — see definition of ϕ^* in Eq. (9). Thus, the distance d_{a_1,a_2} between the aircraft is decreasing as θ increases until $\theta = \phi \leq \phi^*$.

Step 2: Minimum distance for scenario 2 The rate of change in distance with turn angle (the derivative in Eq. 13) becomes zero if $\theta = \phi^*$ which can occur if the heading angle change ϕ desired is greater than ϕ^*. The minimal distance, reached when the turn angle becomes $\theta = \phi^*$ is given by (from Eq. 11)

$$\begin{aligned} d_{a_1,a_2}(\phi^*) \ &= \ \sqrt{(R\sin\phi^*)^2 + (R - R\cos\phi^*)^2} \\ &= \ \sqrt{2R^2(1 - R\cos\phi^*)} \\ &= \ 2R\sin\tfrac{\phi^*}{2} \end{aligned} \tag{14}$$

The Lemma's condition (in Eq. 10) for scenario 2 follows by setting $D_{sep} \leq d_{a_1,a_2}(\phi^*)$ in Eq. (14) and rearranging the terms.

Step 3: Location for minimum distance for scenario 1
The following shows that the minimum distance between two aircraft occurs when both aircraft are on the straight-line segment, equidistant from the curved path. To show this, the distance $d_{a_{11},a_{21}}$ between aircraft a_{11} and a_{21} (general non-equidistant case — see Fig. 7) is compared to the distance $d_{a_{12},a_{22}}$ between aircrafts a_{12} and a_{22} (symmetric, equidistant case) where the distance between a_{12} and point C as well as a_{22} and point B are the same length x.

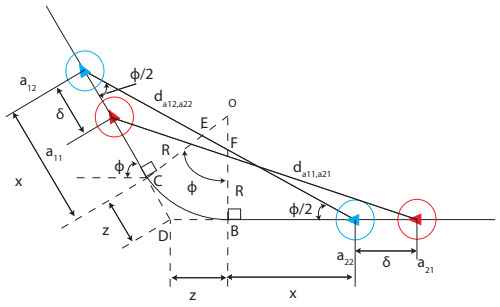

Fig. 7. General distance between aircrafts during single turn when forward aircraft has passed the curved path of the turn. Distance between the aircraft, $d_{a_{11},a_{21}}$, represents the non-equidistant case, and and distance $d_{a_{12},a_{22}}$ represents the symmetric, equidistant case.

By geometry, the angle $\angle CDB$ (shared by triangles $\triangle a_{11}Da_{21}$ and $\triangle a_{12}Da_{22}$) is $\pi-\phi$ since two of the angles in the quadrilateral $CDBO$ are $\pi/2$. Then, the distances between the aircraft, $d_{a_{11},a_{21}}$ (non-equidistant case) and $d_{a_{12},a_{22}}$ (symmetric, equidistant case), can be found by using the law of cosines as shown below.

$$\begin{aligned} d^2_{a_{11},a_{21}} &= d^2_{Da_{11}} + d^2_{Da_{21}} - 2d_{Da_{11}}d_{Da_{21}}\cos(\pi-\phi) \\ &= 2(x+z)^2(1+\cos(\phi)) + 2\delta^2(1-\cos(\phi)) \end{aligned} \tag{15}$$

$$\begin{aligned} d^2_{a_{12}a_{22}} &= d^2_{Da_{12}} + d^2_{Da_{22}} - 2d_{Da_{12}}d_{Da_{22}}\cos(\pi-\phi) \\ &= 2(x+z)^2(1+\cos(\phi)) \end{aligned} \tag{16}$$

The differences between the two distances, the non-equidistant case and the symmetric equidistant case, can be found by subtracting Eq. (15) and Eq. (16) to obtain

$$d^2_{a_{11},a_{21}} - d^2_{a_{12},a_{22}} = 2\delta^2(1-\cos\phi) \geq 0. \tag{17}$$

Therefore, from Eq. (17) the symmetric, equidistant case has the smallest distance for aircraft pairs during the single-turn case under scenario 1. This minimum distance $d_{a_{12},a_{22}}$ can be found by adding the three distances $d_{a_{12}E}$, d_{EF}, and $d_{a_{22}F}$, where distance $d_{a_{12}E}$ is the same as distance $d_{a_{22}F}$ by symmetry.

Step 4: Minimum-distance expression for scenario 1 Note that the travel distance between a_{12} and a_{22} is $\overline{D}$. Since the arc length of the turn, between point B and point C in Fig. 7, is $R\phi$, distance x is found to be $\frac{1}{2}(\overline{D}-R\phi)$. Due to symmetry in geometry, $\triangle OEF$ is an isosceles triangle. Since $\angle EOF$ is the turn angle ϕ, the angles $\angle a_{12}EC$, and $\angle Ea_{12}C$ are found as $\pi/2-\phi/2$ and $\phi/2$, respectively. From the right-angled triangle $\triangle Ea_{12}C$,

$$d_{CE} = d_{BF} = \frac{1}{2}\tan(\phi/2)(\overline{D}-R\phi) \tag{18}$$

$$d_{a_{12}E} = d_{a_{22}F} = \frac{1}{2}\frac{\overline{D}-R\phi}{\cos(\phi/2)}. \tag{19}$$

Since the distances d_{OC}, d_{OB} are the turn radius R, from Eq. (18),

$$d_{OE} = d_{OF} = R - d_{CE} = R - \frac{1}{2}\tan(\phi/2)(\overline{D}-R\phi) \tag{20}$$

Next, from $\triangle OEF$, the distance d_{EF} between points E and F can be found by using the law of sines as

$$\frac{d_{EF}}{\sin\phi} = \frac{d_{OE}}{\sin(\pi/2-\phi/2)}. \tag{21}$$

Substituting for distance d_{OE} from Eq. (20) into the above equation leads to

$$\begin{aligned} d_{EF} &= \frac{(R-\frac{1}{2}\tan(\phi/2)(\overline{D}-R\phi))\sin\phi}{\sin(\pi/2-\phi/2)} \\ &= 2R\sin(\phi/2) - \frac{\sin^2(\phi/2)}{\cos(\phi/2)}(\overline{D}-R\phi) \end{aligned} \tag{22}$$

Then, the minimal spacing between aircraft can be found as $d_{a_{12},a_{22}} = d_{a_{12}E} + d_{EF} + d_{a_{22}F}$ (from Eqs. 19,22)

$$d_{a_{12},a_{22}} = (\overline{D}-R\phi)\cos(\phi/2) + 2R\sin(\phi/2) \tag{23}$$

which results in the condition (in Eq. 9) for scenario 1 of the Lemma by setting $d_{a_{12},a_{22}} \geq D_{sep}$ in Eq. (23) and rearranging the terms. ■

Consecutive Turn Analysis: A general conflict resolution algorithm could have multiple consecutive turns; the conflict-free single turn analysis can be used to show existence of conflict-free multiple turns provided each turn is sufficiently separated from each other, as stated below.

***Lemma 3* (Decoupled Consecutive Turns):** Consider two consecutive turns of a route as shown in Fig. 4 with the straight segments tangential to the curved paths. If conditions of the single turn Lemma 2 are satisfied for each of the turns inside the consecutive turn maneuver shown in Fig. 4, then the consecutive turn maneuver is conflict free as long as the straight segment in between the two turn arcs is sufficiently large.

Proof: The proof follows by choosing a straight line segment $\overline{v_{p1}v_{p2}}$ of length $D_{decouple} \geq \overline{D}$, which decouples the conflicts in the two turns into two single turn cases. ■

Remark 6: A large straight line section between the turns is only used to establish the existence of a conflict-free solution. In practice, this distance should be chosen as small as possible to reduce the space needed for the turn maneuvers.

B. Flow Intersect Procedure

The following Lemma shows that the splitting of each route into three paths allows for a conflict-free intersection.

Lemma 4: Aircraft that arrive synchronized do not have conflicts with each other in the intersection area (marked by D_i in Fig. 2 for Route R_1) with the use of the path assignment procedure in Definition 2 if the path lengths from the arrival points to the straight line segments are all equal.

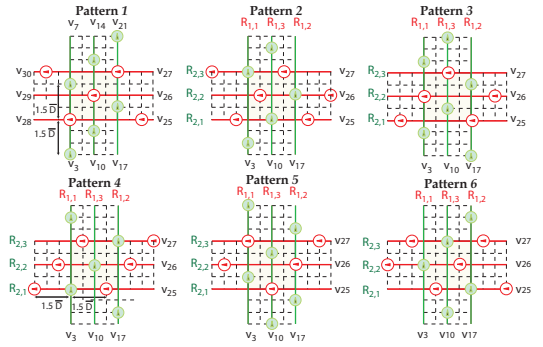

Fig. 8. All possible positions of aircraft whenever an aircraft arrives at a start of the straight line segment of the intersection in Fig. 2.

Proof: If the path lengths from the arrival points to the beginning of the straight line segments (e.g., from v_1 to v_3 or from v_{22} to v_{26} in Fig. 2) are all equal, then all possible positions of other aircraft whenever an aircraft enters a straight line segment are shown in Fig. 8. Some of the potential aircraft positions (at the discrete time instants) shown in Fig. 8 may be empty, i.e., they might not have an aircraft; however, aircraft cannot occupy any other location due to (a) arrival synchronization; and (b) equidistant path lengths to the straight line segments from the arrival points v_1 and v_{22}.

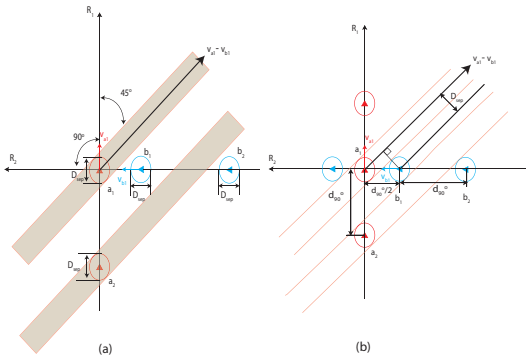

Fig. 9. (a) Relative motion of aircraft a_1 with respect to aircraft b_1 for perpendicularly intersecting flows. (b) Minimum separation d°_{90} between aircraft to avoid conflict using relative motion of aircraft a_1 with respect to aircraft b_1

Let two perpendicularly intersecting route R_1 and R_2 have aircrafts all travel with the same speed as shown in Fig. 9. Each aircrafts within its flow route are separated by distance $d_{90^\circ} > D_{sep}$. The relative motion of aircraft a_1 relative to b_1 is described as $v_{a1} - v_{b1}$, shown in Fig. 9 (a), which is oriented 45 degrees from route R_2 (since all aircrafts travel with the same speed and route R_1 and R_2 are oriented perpendicular to each other). The relative motion of the protection circle centered at a_1 of diameter D_{sep} generates the shaded area in Fig. 9(a). Here, there will be no conflict between the aircrafts if the protective circle centered around aircraft b_1, does not intersect this shaded area, i.e., provided

$$d_{90^\circ} = 2(\frac{D_{sep}}{\sin(45^\circ)}) = 2\sqrt{2}D_{sep} \tag{24}$$

Splitting each route into three paths can enable the spacing between aircraft on each path to be increased by three times (i.e., $3\overline{D}$) which is sufficiently large to develop conflict-free intersections for the perpendicular paths (say, $R_{1,1}$ and $R_{2,1}$ in Fig. 8) since

$$3\overline{D} > 3D_{sep} > 2\sqrt{2}D_{sep} = d_{90^\circ}.$$

■

Thus, the above approach develops a CRP that can be designed in a decentralized manner while accounting for aircraft turn dynamics.

REFERENCES

[1] G. Chatterji, B. Shridar, and K. Bilimoria. En-route flight trajectory prediction for conflict avoidance and traffic management. *AIAA Guidance Navigation and Control Conference, July 29-31, San Diego, CA*, pages 1–11, 1996.

[2] W. B. Cotton. Formulation of the air traffic system as a management problem. *IEEE Trans. on Communications*, 21(5):375–382, May 1973.

[3] K. D. Bilimoria, K. S. Seth, H. Q. Lee, and S. R. Grabbe. Performance evaluation of airborne separation assurance for free flight. *AIAA Guidance Navigation and Control Conference, August 14-17, Denver, CO*, pages 1–9, AIAA 2000–4269, 2000.

[4] A. L. Visintini, W. Glover, J. Lygeros, and J. Maciejowski. Monte carlo optimization for conflict resolution in air traffic control. *IEEE Trans. Intel. Trans. Sys.*, 7(4):470–482, Dec. 2006.

[5] L. Pallottino, E. M. Feron, and A. Bicchi. Conflict resolution problems for air traffic management systems solved with mixed integer programming. *IEEE Trans. Intel. Trans. Sys.*, 3(1):3–11, Mar. 2002.

[6] Z.-H. Mao, D. Dugail, E. Feron, and K. Bilimoria. Stability of intersecting aircraft flows using heading-change maneuvers for conflict avoidance. *IEEE Trans. Intel. Trans. Sys.*, 6(4):357–369, 2005.

[7] C. Tomlin, I. Mitchell, and R. Ghosh. Safety verification of conflict resolution maneuvers. *IEEE Trans. Intel. Trans. Sys.*

[8] Z.-H. Mao, D. Dugail, and E. Feron. Space partition for conflict resolution of intersecting flows of mobile agents. *IEEE Trans. Intel. Trans. Sys.*, 8(3):512–527, September 2007.

[9] S. Devasia, D. Iamratanakul, G. Chatterji, and G. Meyer. Decoupled conflict-resolution procedures for decentralized air traffic control. *IEEE Trans. on Intelligent Transportation Systems*, DOI 10.1109/TITS.2010.2093574:1–16, To Appear 2011.

[10] S. Devasia and G. Meyer. Automated conflict resolution procedures for air traffic management. *Proc. of the 36th Conference on Decision and Control, Phoenix, AZ*, pages 2456–2462, Dec. 1999.

[11] A.M. Bayen, R.L. Raffard, and C.J. Tomlin. Adjoint-based control of a new eulerian network model of air traffic flow. *IEEE Trans. on Control Systems Technology*, 14(5):804–818, September 2006.

[12] H. Erzberger. Design principles and algorithms for automated air traffic management. *AGARD Lecture Series No. 200, Knowledge-Based Functions in Aerospace Systems, San Francisco*, November, 1995.

[13] J. Krozel, C. Lee, and J. S. B Mitchell. Turn-constrained route planning for avoiding hazardous weather. *Air Traffic Control Quarterly*, 14(2):159–182, 2006.